BNL-221195-2021-TECH

NSLSII-ASD-TN-346

Accelerator physics at NSLS-II: research accomplishments in 2020

V. Smaluk

December 2020

Photon Sciences

Brookhaven National Laboratory

U.S. Department of Energy

USDOE Office of Science (SC), Basic Energy Sciences (BES) (SC-22)

DISCLAIMER

NSLS-II TECHNICAL NOTE BROOKHAVEN NATIONAL LABORATORY	NUMBER NSLSII-ASD-TN-346
AUTHORS: V. Smaluk, G. Bassi, A. Blednykh, Y. Li, X. Yang, L.H. Yu, F. Plassard, S. Kongtawong, G. Wang, Y. Hidaka, J. Choi, T. Tanabe, D. Hidas	DATE 12/31/2020
Accelerator physics at NSLS-II: research accomplishments in 2020	

Accelerator physics at NSLS-II: research accomplishments in 2020

V. Smaluk, G. Bassi, A. Blednykh, Y. Li, X. Yang, L.H. Yu,
F. Plassard, S. Kongtawong, G. Wang, Y. Hidaka, J. Choi,
T. Tanabe, D. Hidas

Dec. 31, 2020

Abstract

NSLS-II accelerator physicists provide scientific support for user operations, as well as for improvements and developments of the accelerator systems. This work includes optimization of the NSLS-II performance with high beam current and low vertical emittance, improvement of the beam stability, development of new software tools for operations and beam studies. The accelerator physicists productively worked on a number of research activities such as the conceptual design of NSLS-II accelerator upgrade; design and optimization of advanced low-emittance lattices; development of novel methods to study nonlinear beam dynamics; ultrafast electron diffraction and microscopy. The physicists also contributed to the BNL electron-ion collider project, to the APS and ALS upgrade projects. Research accomplishments achieved in 2020, are summarized in this report.

1 Introduction

In 2020, the top priority of the NSLS-II accelerator physicists working in the Accelerator Physics Group, Accelerator Coordination Group, and Insertion Devises Group, was the scientific support of the NSLS-II user operations. Although the COVID-19 pandemic affected our work making it more difficult, the machine continued to operate reliably with high performance. The accelerator physicists also worked on several projects to further improve the beam quality and machine reliability. A beam current of 500 mA was successfully demonstrated with a stable beam and 8 hours of beam lifetime. The machine was optimized with a new working point to stabilize the beam size with a vertical emittance of 8 pm·rad. A dedicated cell controller has been implemented to monitor the beam stability, the data are used to identify abnormal high-frequency motion and to pinpoint a source of the perturbation. Possible use of the pinger to compensate the top-off injection transient was explored. To explore a potential operation mode for time-resolved experiments, characterization of beam parameters and study of beam-induced heating were carried out. New PyElegant software for linear and nonlinear lattice characterization and optimization was developed. A model-independent optimization of the Injector was implemented. New techniques based on Machine Learning have been developed: a neural-network-assisted method for optimization of nonlinear beam dynamics and a tool for detection of anomalies to improve the machine reliability and performance.

In addition to supporting the facility operations and developments, the NSLS-II accelerator physicists were engaged in a number of R&D activities. The LDRD project 17-015 "NSLS-II High Brightness Upgrade and Design Studies" has been successfully completed. A new LDRD project 20-041 "Conceptual Design Options for Future Upgrade of NSLS-II Facility" has been approved and funded, the physicists are working on the concepts of NSLS-II accelerator upgrade. In the framework of the LDRD 19-016, the physical and engineering design of the ultrafast electron microscope has been completed, the project is in the manufacturing stage, the installation and commissioning are scheduled for next year. Under a few memorandums of understanding, the accelerator physicists also contributed to the project of BNL electron-ion collider and to the APS and ALS upgrade projects.

A list of projects and activities is presented below.

- Software tools for beam studies and operations.
- Study of nonlinear beam dynamics.
- Lattice with high chromaticity.
- Assessment of superconducting wiggler for HEX beamline.
- Improvement of beam diagnostic instruments.
- AC local orbit bumps.
- Study of longitudinal beam dynamics and support of RF system.
- Online optimization of beam injection.
- Novel techniques for nonlinear lattice optimization.
- Collective effects and impedances.
- Conceptual design options for NSLS-II upgrade.
- Theoretical studies of free-electron lasers.
- Ultra-fast electron diffraction and microscopy.
- Study of longitudinal beam dynamics and RF system for EIC.
- Impedance studies for EIC.
- Lattice optimization for EIC.
- Beam-based tests of the ALS-U bellows and APS-U stripline.

Some results of the research and developments carried out by NSLS-II accelerator physicists in 2020 are briefly described in the next chapters.

2 Software tools for beam studies and operations

The common tools package is now a complete set of Python scripts and notebooks for measurement and correction of the Storage Ring betatron tunes, chromaticity, lattice functions, coupling, and orbit; characterization of nonlinear beam dynamics; DC and AC local orbit bumps; Injector controls; interface to the bunch-by-bunch feedback system; interface to the fast orbit feedback system [1]. In FY20, the HLA common tools were converted from Python 2 to Python 3 because Python 2 support ended in January 2020 and serious security vulnerabilities can be discovered in the future. The routine characterization of Storage Ring lattice using the common tool software was already found to be helpful for understanding the long-term evolution of the machine. The development of a "single-button" tool for fast lattice characterization using BPM turn-by-turn data is complete. The Python script with a simple CSS interface is designed for regular lattice characterization by operators during the machine start-up. The measured data will be used for routine tracking of the Storage Ring lattice. Both the python code and the CSS page were tested with the beam and the tool is now ready to train the operators. The HLA common tools program is further evolved to the development of Python Middle Layer (PyML) with the same or better functionality as Matlab Middle Layer (MML) used for accelerator controls at most of the light sources worldwide. The idea is to develop a set of Python functions, which can be used from a python command line, function, notebook, or script. This work is started with an upgrade of the aphla (Accelerator Physics High-Level Applications) Python package that was developed during the NSLS-II project. This package contains about 30 Python functions similar to the MML ones. However, the core functions have been frozen since 2016. We plan to develop, test, and debug Python functions using lattice models based on the input file in ELEGANT format and provide built-in help and a detailed manual for every function.

3 Study of nonlinear beam dynamics

The amplitude-dependent shift of betatron tunes caused by the machine nonlinearity was regularly measured since 2015. The data collected from 2015 to 2020 were systematically analyzed in comparison with the lattice model, both for the bare lattice and the lattice with 3 damping wigglers [2]. First, simulation scans of energy and sextuplets were carried out and the data were fit to second-order polynomials. Then the measured data were fit to the polynomials too. The result shows the long-term drift of the tune-amplitude dependence was dominated by the energy change and the effect of sextupoles was found small. This conclusion contradicted the measured history of the RF frequency and of the sum of orbit correctors' strength and became a mystery for our model of the NSLS-II lattices. As it was found, the formulae describing the relation between the RF frequency and machine circumference, and the relation between the beam energy and the sum of correctors' strength neglected the important contribution of the ground movement and circumference change. The modified relations with the circumference change taken into account, show that small variations of the circumference can produce a large effect on the tune-amplitude dependence, similar to that caused by the energy variation even though if the energy does not change. This result gives a reasonable interpretation for the large observed long-term variations of the amplitude-tune dependence, and points out a direction of further study: we need to monitor a seasonal change of the RF frequency and the orbit correctors' strength. The development of an advanced algorithm for orbit correction and RF feedback would result in better long-term beam stability.

The multi-frequency AC LOCO (Linear Optics from Closed Orbits) technique was further developed to study nonlinear beam dynamics [3]. This technique is based on the simultaneous beam excitation by sinewave signals with multiple frequencies using several fast correctors. The unique combination of the fast speed and high measurement accuracy provides an opportunity to measure both the misalignment and the field-offset errors of sextupoles. Beam excitation via fast correctors results in the elimination of the systematic error caused by the hysteresis effect. Systematic errors of the sextupole alignment caused by the orbit drift and the power supply calibration are also eliminated because the measurement takes only two minutes and does not depend on the current-to-field conversion of the sextupole magnets. Furthermore, the simulation studies indicate that the multi-frequency AC LOCO together with an orbit bump bigger than 0.5 mm can be applied to measure the relative field offset of a sextupole magnet with a precision better than 10%. The measurement technique was experimentally tested at the NSLS-II Storage Ring.

4 Lattice with high chromaticity

High chromaticity provides fast damping of coherent beam oscillations and helps to suppress collective beam instabilities so the gain of the bunch-by-bunch feedback can be reduced. This is helpful for stable operation with low vertical emittance and for the special fill pattern with high-intensity bunches required for time-resolved experiments. For both the bare lattice and the lattice with all damping wigglers and undulators, high-chromaticity options were developed and optimized by computer simulations. The bare lattice with the chromaticity of 7 (both horizontal and vertical) was proved good by a beam test: 7.9 mA of beam current in a single bunch was accumulated without feedback, the beam intensity was limited by vacuum rather than the beam instability. For the operational lattice with chromaticity +7/+7, the horizontal dynamic aperture was lower than for the regular operational lattice, the injection was possible but with low efficiency. Applying the RCDS optimization of harmonic sextupoles, we were able to improve the injection efficiency up to 85-90%. This lattice was successfully tested with the bunch-by-bunch feedback gain reduced by 6 dB horizontal and by 12 dB vertical. 400 mA of the beam current was accumulated, the vertical emittance was 8 pm with negligible excitation by the feedback. With high chromaticity and lowered BBFB gain, the beam current of 11.3 mA was accumulated in the single-bunch mode, the beam intensity was limited by vacuum.

5 Superconducting wiggler for HEX beamline

A superconducting wiggler (SCW) is planned to be installed in cell 27 of the NSLS-II Storage Ring for the HEX beamline. Interaction of the electron beam with the resistive-wall impedance of the low-gap SCW liner and with the geometric impedance of the transition sections results in excitation of electromagnetic fields, dissipation of which heats the vacuum chamber in the cold volume. The beam-induced heat power resulted from the beam interaction with the geometric and resistive-wall impedance (including normal and anomalous skin effects) was estimated using analytical formulae and numerical simulations for two design options with new vacuum chamber geometry: one from the vendor and one from NSLS-II [4]. Combining the contributions from the cold liner, two warm tapered transitions, and two transitions from 300 K to 20 K, we estimated the total beam-induced power in the HEX SCW. For the r.m.s. bunch length of 3 mm and the beam current of 500 mA in 1000 bunches, the total power is about 30 W (NSLS-II design) and about 75 W (vendor design). It was also noted that having bellows in the cold volume proposed in the vendor design can be dangerous. In a possible case of poor contact in the RF shield fingers, an arc will occur or the beam will interact with the "unshielded" bellows having much higher impedance than the RF-shielded one. Any of these effects can suddenly increase the heat load resulting in quenches. The beam stay-clear with the low-aperture HEX chamber was also estimated. The vertical dynamic aperture is reduced from 3.5 mm (limited by the damping wigglers) to 2.5 mm, the horizontal aperture does not change much.

6 Improvement of beam diagnostic instruments

We carried out a series of studies of the X-ray pinhole cameras installed to measure the beam emittance using radiation from the bending magnet and 3-pole wiggler (3PW). The studies were motivated by an observed discrepancy in the emittance measured by these two devices. Simulations done with the SRW code show that the optimum pinhole size is about $20-25$ μm. A new set of round pinholes with a diameter of 10, 30, 75, and 100 μm was manufactured and installed in the 3PW device. Measurements with the beam show consistent results for both devices in the vertical plane. However, in the horizontal plane, the images seem to be sensitive on the alignment, especially when the pinhole size is small. It was confirmed by simulations that a rectangular pinhole is not sensitive to the misalignment but a circular pinhole is very sensitive to the misalignment for both planes. The disagreement in the horizontal beam size measured with different pinhole sizes could come from the insufficient photon flux reduced by small pinholes, therefore the measured beam size is underestimated. So the optimum horizontal pinhole size should be 100 to 150 μm to provide less than 5% error and the optimum for the vertical size is 22 μm (can be 20 to 25 μm). We found the pinhole point spread function is nearly independent of the photon energy and the filters for varying photon energies will likely have no significant influences on the resolution of beam size measurements, if the pinhole size exceeds 30 μm. The experimental comparison of the effect of the filter placed upstream and downstream the pinhole is about 2% in the horizontal plane and 5% in the vertical plane, the downstream filter gives a smaller size.

7 AC local orbit bumps

Generation of AC orbit bumps using fast correctors was developed at NSLS-II for accelerator physics studies. The use of narrow-band signals for the beam excitation and measurements using synchronous detection allows us to achieve high sensitivity and a good signal-to-noise ratio. The AC bumps localized at light-generating insertion devices (ID) are considered by NSLS-II beamline scientists as a possible user operation mode [5]. Transverse oscillations of the electron beam in selected light-generating insertion devices result in the controllable motion of the X-ray beam in the beamlines. The beam excitation system is expected to serve multiple beamlines providing individually customized beam motion. This feature would be beneficial for NSLS-II user programs including the experiments where X-ray scanning is needed. Before the implementation of the AC orbit bumps into user operations, we investigated if the residual perturbation of the electron beam affects the other beamlines. Software tools for pre-calculating the angle and position bumps were developed and implemented. Both positional and angular AC bump was created and well localized in the CSX and/or FXI beamlines and the effect of this AC bump on other beamlines was studied. As it was found, the Fast Orbit Feedback can effectively suppress the residual perturbation in the frequency range up to 50 Hz with the AC excitation amplitude up to 13 μrad. The beamlines determine whether the achievable amplitude of the AC orbit bump is sufficient or not. If there is a strong interest in the NSLS-II user community, an upgrade of the fast correctors' power supplies is possible to increase the amplitude of beam excitation.

8 Study of longitudinal beam dynamics and support of RF system

A realistic model of the RF system is essential to simulate the longitudinal beam dynamics with three main RF cavities (the 3rd RF system will be commissioned next year) and 3rd-harmonic cavities. A model of the Low-Level RF feedback (LLRF) has been implemented into the SPACE code for self-consistent simulations of beam loading effects. It is important to take into account the transfer functions of all the components in the full feedback loop. Transfer functions of the NSLS-II RF system with two and three cavities were studied and modeled. Impacts of various combinations of the proportional and integral coefficients on the RF cavity field amplitude response were analyzed. The simulation results were compared with the beam-based measurements. Beam synchronous phase as a function of the voltage step jump or drop was measured at 100 mA and 150 mA of the beam current with the LLRF feedback loop open and closed. All measured data show good agreement with the SPACE simulation.

9 Online optimization of beam injection

The Facility Improvement Project (FIP) "Methods of online optimization of NSLS-II storage ring concurrent with user operations" is dedicated to improving the beam quality for user experiments. The expected benefits for the NSLS-II user community are reduced top-off injection frequency, improved beam stability, and minimized orbit perturbation during the injection. One of the goals of the FIP is to reduce the injection transient down to a level transparent to the beamline users. Minimizing the beam perturbation during injection is realized by the online optimization of the injection kickers. First applications of the Robust

Conjugate-Gradient Algorithm resulted in a reduction of the beam oscillation amplitude after injection by a factor of 6. The upgrade of the Injector hardware is needed for further reduction of the injection transient. After the timing jitter of the injection kickers was fixed, we pursue the original plan of the kicker upgrade with the adjustable pulse width. A prototype of the tuning slot activated by a step motor to vary the inductance, and therefore the width of the kicker pulse, was installed and tested. A 64-ns tuning range meeting the specification was achieved. The control software has been developed and tested [6]. Optimization of the NSLS-II sextupoles using RCDS was successfully applied to increase the dynamic aperture of the newly developed high-chromaticity lattice.

10 Novel techniques for nonlinear lattice optimization

A forward-reversal integration technique has been developed and applied to fast dynamic aperture optimization for storage rings [7, 8]. The fundamental principle of this method is the numerical characterization of the sensitivity of a chaotic motion to its initial conditions by using round-off errors. An indicator of chaotic motion of the charged particle can be obtained by comparing the forward integrations of the particle trajectory with corresponding reversal or "backward" integration. For a chaotic trajectory, cumulative round-off errors of numerical integration are scaled, which results in an exponential growth of the difference between the forward and reversal integration. This exponential effect is a generic chaos indicator representing the sensitivity of chaotic motion to its initial conditions. The indicator is observable even through short-term particle tracking simulations, so it gives an early sign of the chaos in the beam motion in a storage ring. Therefore, adopting it as an objective function can speed up the optimization of dynamic aperture. The NSLS-II storage ring and a test MBA lattice were used as examples to illustrate the application of this method. The method has been included in the ELEGANT code as the chaos_map command [9].

A new approach of non-linear lattice correction has been developed. It is based on the general minimization of high-order geometrical effects using octupoles. Optimization of the position and phase of the octupoles with respect to the chromatic sextupoles is carried out to provide a simultaneous correction of the tune shift with amplitude and systematic minimization of all geometrical phase-dependent driving terms of the same order. This scheme has been analyzed using a simple FODO lattice model and applied to several lattice options for the future low-emittance upgrade of NSLS-II. For every case, the on-momentum dynamic aperture has been significantly improved without the use of numerical optimization tools.

11 Collective effects and impedances

An intensity-dependent increase of the beam emittance, energy spread, and bunch length below the microwave instability threshold was observed at NSLS-II. The bunch length was measured by a streak camera, the energy spread was measured by a synchrotron light monitor installed in a dispersive section, and the emittance was measured by an X-ray pinhole camera. This growth of the 3D beam emittance results from a combined effect of the intra-beam scattering (IBS) and beam-impedance interaction. In the case of a low-emittance ring with medium energy of 3 GeV, none of these effects is dominant. Numerical simulations of the beam dynamics were carried out using ELEGANT code taking both the IBS and impedance into account, the simulation results are consistent with the measured data. A summary of these studies was presented at the 8th Low Emittance Rings Workshop [10].

The beam-induced heating of the stripline kicker was studied experimentally, theoretically, and numerically [11]. A diagnostic stripline for the experimental study of beam-induced heating has been designed, manufactured, and installed in the NSLS-II storage ring. The electrode temperature of the diagnostic stripline was measured as a function of the beam current by an infrared camera through six viewports. The beam-induced power was calculated using the actual beam parameters and the loss factor computed by 3-D electromagnetic simulations. Lambertson and Shafer formalisms for the longitudinal and transverse impedances of a simplified stripline geometry were compared with numerical results, a frequency range, within which the analytical approach can be applied, was found. We estimated the local temperature by simulations using the ANSYS finite-element code for the considered geometry with the beam power loss as an input. The experimental and numerical results are in reasonable agreement, thus validating the right impedance model used. The measured temperature dependence on the number of bunches was also consistent with the theory.

12 Conceptual design options for NSLS-II upgrade

The LDRD project 17-015 “NSLS-I High Brightness Upgrade Design Studies” is complete. The Triple-Bend Achromat (TBA) lattice design for the future NSLS-II brightness upgrade was summarized in the LDRD final report. This lattice provides 300 pm·rad horizontal emittance, it can be further reduced to below 200 pm·rad with additional damping wigglers. The layout of the TBA lattice is perfectly fitted into the existing storage ring tunnel and beamlines. Many present NSLS-II magnets can be re-used, including 30 dipoles. The dynamic aperture is sufficient for the conventional off-axis top-off injection. A large energy acceptance ensures a sufficiently long beam lifetime.

A new LDRD 20-041 project “Conceptual Design Options for Future Upgrade of NSLS-II Facility” has been approved and funded. This LDRD would deliver a pre-conceptual design for the NSLS-II upgrade, which, once implemented, will result in a large gain in the facility performance compared to today’s operations. We will develop a set of lattice designs together with the assessment of the required changes in the NSLS-II accelerators and subsystems.

Supported by the LDRD funding, we are assessing three machine upgrade options, which would fit into the existing infrastructure:

- A medium-scale upgrade to the accelerator that would result in incremental improvements in brightness;
- High-flux upgrade with the beam current of 2 A and the horizontal emittance of 100 pm·rad;
- Low-emittance upgrade with the beam current of 500 mA and the horizontal emittance of 20 pm·rad at the energy of 3 GeV. We are also considering the beam energy up to 4 GeV, which is motivated by a large step in the capabilities of IDs with the same magnet gap.

Currently, three lattice options for the low-emittance upgrade are being developed: 1) hybrid 7BA lattice based on the ESRF-EBS approach providing 31 pm emittance; 2) Double Complex Bend Achromat (DCBA) upgrade lattice providing 25 pm emittance; 3) Triple Complex Bend achromat (TCBA) lattice providing 35 pm emittance.

The upgrades paths that are currently being considered, the potential benefits to the scientific community, and the technical challenges that we can expect are summarized in the White Paper.

13 Theoretical studies of free-electron lasers

A theoretical basis to study the conditions for a hard X-ray FEL oscillator based on the electron beam in the medium energy range from 3 to 4.5GeV has been developed [12]. As it was found, the approach previously developed for the small-signal low gain formula can be modified so that the gain can be derived without the originally adopted "no focusing approximation", and a strong focusing can be applied. The new formula allows the gain calculation with harmonic lasing. In this formula, the gain is a product of two factors with one of them depending only on the harmonic number, and period and gap of the undulator. It was shown that it is favorable to use harmonic lasing to design a hard X-ray FEL working in the medium energy range and in the small-signal low gain regime. Several examples were studied to assess the principal possibility of an XFEL option for the NSLS-II upgrade. These examples indicate a hard X-ray FEL in the medium-energy range seems possible, even though it sets rather challenging conditions for the storage ring.

The dynamics of an isolated spike of radiation in the superradiant regime have been studied [13]. Certain conditions were found where the pulse moves with a group velocity larger than the velocity of light in vacuum and is followed by a tail resulting from complex postsaturation dynamics. The tail looks like a train of subpulses with both transverse and longitudinal coherence and decaying amplitudes. The dynamical conditions leading to the formation of the main pulse and the tail were analyzed. The correlation of the tail structure with the longitudinal phase space of the electrons was studied and a way to partially suppress this tail was found.

14 Ultra-fast electron diffraction and microscopy

The LDRD project 19-016 "Demonstration of feasibility of sub-nm, picosecond electron microscope for the life sciences" is close to the final stage. The lattice and component specifications were completed allowing the mechanical design to proceed. The comments from the Preliminary Design Review were incorporated into the design. All components of the UEM beamline are mounted on a single mounting plate, the beamline is an integrated system that can be installed as a single component. This design provides an easy change from UED to UEM and back, reduces residual magnetic fields, keeps the original vacuum chamber components clear, and maintains the original distance from the gun to the detector. Most components of the UEM beamline has been manufactured, we scheduled the installation and commissioning in 2021. As a part of the preparation for the electron microscope commissioning, we have proposed, planned, and completed an experiment to measure the shot-to-shot energy jitter of the UED beam. We have proposed and developed a concept of a unique monochromator providing extremely low energy spread of MeV electron beam for ultrafast electron diffraction and microscopy [14]. The monochromator can significantly improve the UED/UEM performance minimizing the energy spread in the single-shot mode and the shot-to-shot energy jitter in the accumulation mode demanded by high electron flux applications. The Bragg-Diffraction method of the in-situ electron beam diagnostics has been reported at the 11th International Particle Accelerator Conference as a contributed talk [15].

15 Longitudinal beam dynamics and RF system for EIC

In the frameworks of MOUs, the NSLS-II accelerator physicists made significant contributions to the BNL Electron-Ion Collider R&D including computation of the impedance, studies of longitudinal beam dynamics and assessment of the RF system configuration, linear and nonlinear lattice optimization.

Analytical estimates and computer simulations of transient beam loading have been done for the EIC electron storage ring. A stable configuration of the main RF system at 10 GeV was found: 18 single-cell cavities with reverse phasing (13 focusing and 5 defocusing). An encouraging solution with higher-harmonic cavities was also found: 5 asymmetric HHCs: 3 for bunch lengthening and 2 for bunch shortening to improve stability. Active HHCs are also considered. However, the transient is too large, an alternative way to reduce the heat load is the doubling the number of bunches from 580 to 1160, then the HHC might not be needed. Results of these studies were discussed at telemeetings and will be incorporated in the EIC conceptual design report.

16 Impedance studies for EIC

Studies of impedances and beam intensity limitations for the EIC were carried out under an MOU, preliminary results were reported at the workshop “SuperKEKB: Challenges for the high luminosity frontier” [16]. The studies include preliminary estimates of the impedance budget for the EIC electron ring, comparison with PEP-II and SuperKEKB colliders, geometry optimization for the regular vacuum chamber, design of the beam interaction chamber with minimum impedance. Since protons have no radiation damping the residual oscillations of the electron beam are a matter of concern. As it was found, transverse instabilities are damped by the beam-beam tune spread. Longitudinal feedback is needed to suppress the instability caused by high-order modes of the RF cavities. The vacuum requirements were estimated to prevent ion-driven instabilities. A detailed impedance budget of the EIC vacuum chamber is being computed using 3D electromagnetic simulations.

17 Lattice optimization for EIC

The forward-reversal integration has been proved efficient in optimizing the dynamic aperture for light source rings, which usually have a multi-fold periodical lattice structure. This approach has been also used to optimize the dynamic aperture of the future electron-ion collider's electron ring [17]. Unlike the light sources, the EIC lattice includes one or two interaction points where the lattice functions are very different from the rest of the ring. It was found that a single-turn forward-reversal integration provides insufficient information for the optimizer. Increasing the number of tracking turns up to 16 resulted in a much clear difference between good lattice candidates (particles have regular motions) and bad ones (chaotic motions).

18 Beam-based tests of the ALS-U bellows and APS-U stripline

NSLS-II accelerator physicists provided scientific support for the beam-based tests of the ALS-U bellows and APS-U stripline at NSLS-II. For each of these components, the temperature was estimated before the beam studies as a function of the beam current, using the numerical and analytical approach. The temperature was then measured as a function of the beam current. The RF Voltage was also varied to monitor the temperature dependence on the bunch length. The experimental data were compared with the simulations, the results are in good agreement. The measurements of local impedance with and without the components being tested were carried out to be compared with the numerical simulations. As a result of the test, a couple of changes were made in the ALS-U bellows design to reduce the beam-induced heating.

19 Summary

In 2020, the physicists working in the Accelerator Physics Group, Accelerator Coordination Group, and Insertion Devises Group, were providing scientific support for NSLS-II operations and improvements. This includes the following activities: studies of nonlinear beam dynamics [2, 3]; development of a high-chromaticity lattice for NSLS-II; assessment of the superconducting wiggler for HEX beamline [4]; support of improvement of the X-ray pinhole camera; development of the AC orbit bump for beam studies and operations [5]; support of RF system development; online optimization of beam injection (FIP) [6]; improvement of orbit feedbacks [18]; development of the beam fill patterns with high-current bunches for time-resolved experiments; optimization of the storage ring to provide stable operation with a beam current of 500 mA and vertical emittance of 8 pm-rad; implementation of routine monitoring of the beam stability performance. Significant effort was spent on the development of software tools for operations and beam studies: HLA common tools package [1], PyElegant for lattice characterization and optimization, a novel neural-network-assisted method for nonlinear dynamics optimization, a machine learning tool to detect anomalies.

In parallel, the accelerator physicists were productively working on the following research topics: development of novel techniques for nonlinear lattice optimization [7, 8, 9], studies of collective effects and impedances [10, 11], theoretical studies of free-electron lasers[12, 13]. In the frameworks of a new LDRD, we are working on the conceptual design options for the NSLS-II upgrade, current results of lattice design, beam dynamics studies, and engineering aspects of the upgrade, potential benefits to the scientific community, and the technical challenges are summarized in the White Paper. The ultra-fast electron microscopy LDRD project is close to the final stage [14, 15], the installation and commissioning are planned for 2021.

In frameworks of a few MOUs with the Electron-Ion Collider Directorate, the Accelerator Physics group contributed to the BNL electron-ion collider project [16, 17]. Scientific support for the beam-based tests of the ALS-U bellows and APS-U stripline at NSLS-II was also provided.

The main results have been published in peer-reviewed journals. Unfortunately, participation in the international conferences and workshops in 2021 was very limited by the COVID-19 pandemic, many events have been canceled. However, some results were remotely presented at the 11th International Particle Accelerator Conference [15] and at the 8th Low Emittance Rings Workshop [10, 19, 20]. Figure 1 shows the statistics of journal articles and conference reports published by NSLS-II Accelerator Physics Group in FY14-FY20.

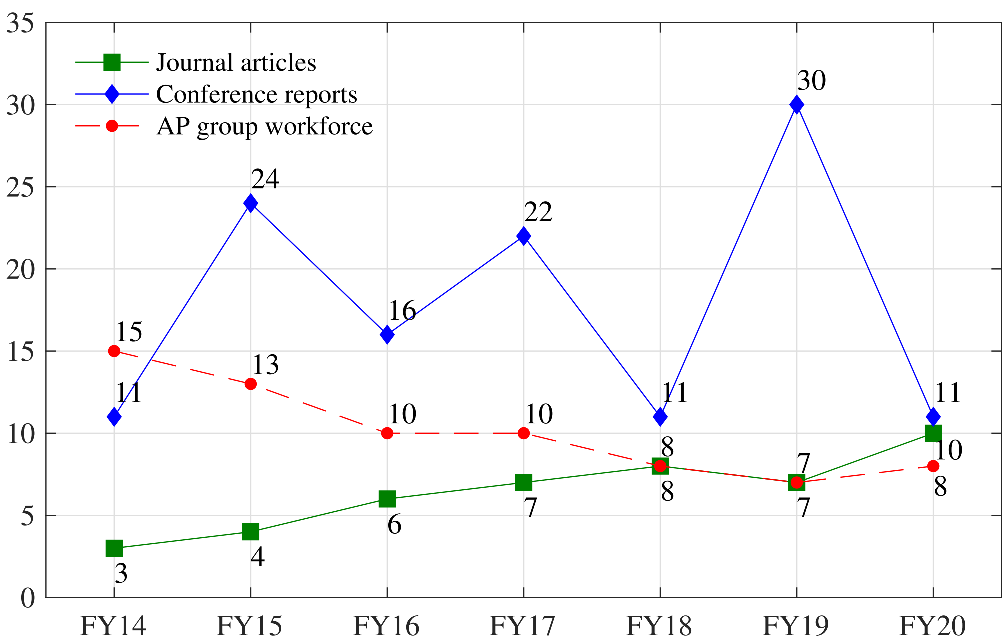

Figure 1: Number of journal articles and conference reports published by the NSLS-II Accelerator Physics group in FY14-FY20.

References

[1] https://gitlab.nsls2.bnl.gov/hlatools.

[2] L.H. Yu, G. Bassi, Y. Hidaka, B. Podobedov, V. Smaluk, G. Wang, X. Yang, Comparison of Amplitude Tune Dependence of NSLS-II Lattices with Models and its Relation to Long Term Circumference Change, BNL-219889-2020-TECH.

[3] X. Yang, V. Smaluk, L. Yu, K. Ha, Y. Tian, Applying Multi-frequency AC LOCO for Finding Sextupole Errors, BNL-219897-2020-TECH.

[4] V. Smaluk, A. Blednykh, C. Hetzel, T. Tanabe, Beam-induced Power in HEX Superconducting Wiggler, BNL-215891-2020-TECH.

[5] X. Yang, V. Smaluk, Y. Tian, K. Ha, C. Mazzoli, W.K. Lee, FOFB-compatible AC Local Bump as a Potential New Operations Mode for NSLS-II, BNL-219882-2020-TECH.

[6] X. Yang, S. Buda, D. Durfee, G. Wang, L.H. Yu, V. Smaluk, T. Shaftan, Progress in Online Optimization of NSLS-II Dynamic Aperture and Injection Transient, BNL-219881-2020-TECH .

[7] Y. Li, Y. Hao, K. Hwang, R. Rainer, A. He, A. Liu, Fast Dynamic Aperture Optimization with Reversal Integration, BNL-215949-2020-TECH.

[8] Y. Li, Y. Hao, K. Hwang, R. Rainer, A. He, A. Liu, Fast dynamic aperture optimization with reversal integration, Nucl. Instrum. Meth. A 988 (2021) 164936.

[9] User's Manual for elegant, 7.13 chaos_map.

[10] A. Blednykh, Combined Effect of IBS and Impedance on the Longitudinal Beam Dynamics, 8th Low Emittance Rings Workshop, Frascati, 2020.

[11] A. Blednykh, B. Bacha, G. Bassi, C. Hetzel, B. Kosciuk, D. Padrazo, T. Shaftan, V. Smaluk, T. Ha, Beam impedance and heating analysis of the diagnostic stripline, Nucl. Instrum. Meth. A 963 (2020) 163729.

[12] L.H. Yu, Medium Energy Hard X-ray FEL Gain, BNL-219843-2020-TECH.

[13] X. Yang, N. Mirian, L. Giannessi, Postsaturation dynamics and superluminal propagation of a superradiant spike in a free-electron laser amplifier, Phys. Rev. Acc. Beams 23 (2020) 010703.

[14] X. Yang, W. Wan, L. Wu, V. Smaluk, T. Shaftan, Y. Zhu, Toward monochromated sub-nanometer UEM and femtosecond UED, Scientific Reports 10 (2020) 16171.

[15] X. Yang, J. Li, M. Fedurin, V. Smaluk, L. Yu, L. Wu, Y. Zhu, T. Shaftan, W. Wan, A Novel Nondestructive Diagnostic Method for Mega-Electron-Volt Ultrafast Electron Diffraction, presented at the 11th Int. Particle Accelerator Conf. (IPAC'20), CAEN, FRANCE, May 2020, paper WEVIR16.

[16] A. Blednykh, Impedance Optimization for EIC, SuperKEKB: Challenges for the high luminosity frontier, Tsukuba, 2020.

[17] Y. Li, Using Forward-Reversal Integration to Optimize EIC's e-ring Dynamic Aperture, BNL-219894-2020-TECH.

[18] S. Kongtawong, Y. Tian, X. Yang, K. Ha, L.H. Yu, T. Shaftan, Recent improvements in beam orbit feedback at NSLS-II, Nucl. Instrum. Meth. A 976 (2020) 164250.

[19] V. Smaluk, Effect of undulators on the lattice, emittance, and energy spread of NSLS-II, 8th Low Emittance Rings Workshop, Frascati, 2020.

[20] Y. Li, Fast dynamic aperture optimization with reversal integration, 8th Low Emittance Rings Workshop, Frascati, 2020.